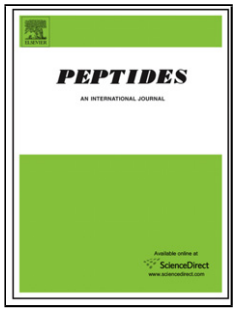

Title: Discovery of a long-acting glucagon-like peptide-1 analog with enhanced aggregation propensity

Authors: Mitsuaki Takeuchi, Masayuki Okamoto, Ryuji Okamoto, Hiroshi Kinoshita, Yu Yamaguchi, Nobuhide Watanabe

PII: S0196-9781(18)30022-6
DOI: https://doi.org/10.1016/j.peptides.2018.01.014
Reference: PEP 69919

To appear in: *Peptides*

Received date: 9-12-2017
Revised date: 24-1-2018
Accepted date: 25-1-2018

Please cite this article as: Takeuchi Mitsuaki, Okamoto Masayuki, Okamoto Ryuji, Kinoshita Hiroshi, Yamaguchi Yu, Watanabe Nobuhide.Discovery of a long-acting glucagon-like peptide-1 analog with enhanced aggregation propensity.*Peptides* https://doi.org/10.1016/j.peptides.2018.01.014

Discovery of a long-acting glucagon-like peptide-1 analog with enhanced aggregation propensity

Mitsuaki Takeuchi[a], Masayuki Okamoto[a], Ryuji Okamoto[a], Hiroshi Kinoshita[a], Yu Yamaguchi[a], and Nobuhide Watanabe[a,b,*]

[a] Mie Research Laboratories, Sanwa Kagaku Kenkyusho, Co., Ltd., 363 Shiosaki, Hokusei-cho, Inabe-city, Mie 511-0406, Japan

[b] Licensing & Business Development, R&D Strategy Center, Sanwa Kagaku Kenkyusho, Co., Ltd., Mitsui Building No.2 5F 1-1Nihonbashi-Muromachi 2-Chome, Chuo-ku, Tokyo 103-0022, Japan

Graphical abstract

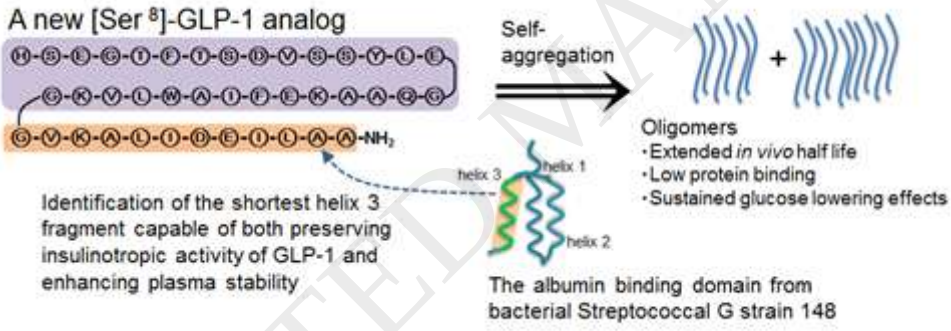

Highlights

- · [Ser^8]-GLP-1(7-35)-GVKALIDEILAA-NH_2 was found as a new long-acting GLP-1 analog.
- ·Our experiments suggest that this GLP-1 analog remains oligomeric in the circulation.
- ·The newly discovered GLP-1 analog has potent long-acting therapeutic effects in diabetic mice.

ABSTRACT: In the course of our search for new GLP-1 analogs, we screened a number of [Ser^8]-GLP-1 analogs using the C-terminal helix 3 of the albumin binding domain 3 of protein G from bacterial Streptococcal G strain 148 (G148-ABD3) as appendage. Our efforts led to the discovery of [Ser^8]-GLP-1 (7-35)-GVKALIDEILAA-NH_2, peptide **6**, as a long-acting GLP-1 analog with enhanced self-associated aggregation. Peptide **6** showed enhanced stability in rat and human plasma and an extended half-life of 5.4 h with good bioavailability in rats and subsequently prolonged therapeutic effects in diabetic mice. Analytical ultracentrifugation and TLC suggest that **6** remains oligomeric in the circulation, which accounts for its extended in vivo half-life. The present work shows the possible enhancement of medium-sized oligopeptides aggregation propensity and highlights the potential advantages of peptide aggregates for long-acting peptide drugs.

Abbreviation: ABD3, albumin-binding domain 3; ACN, acetonitrile; AUC, area under the curve; BA, bioavailability; cAMP, cyclic adenosine monophosphate; CHO, chinese hamster ovary; DIEA, diisopropyl ethylene diamine; C_{max}, peak plasma concentration; CL_p, plasma clearance; DMF, dimethyl formamide; DPP-IV, dipeptidyl peptidase-IV; ELISA, enzyme-linked immunosorbent assay; EMA, European Medicines Agency; FBS, fetal bovine serum; G148-ABD3, albumin binding domain 3 of protein G from the bacterial Streptococcal G strain 148; GLP-1, glucagon-like peptide-1; GLP-1R, GLP-1 receptor; HBSS, hanks-balanced salt solution; HBTU, O-(1H-benzotriazol-1-yl)-N,N,N',N'-tetramethyluronium hexafluorophosphate; HEPES, 4-(2-hydroxyethyl)-1-piperazine ethane sulfonic acid; HPLC, high performance liquid chromatography; HSA, human serum albumin; KRH, Hepes-Krebs ringer; LC/MS, liquid chromatography/mass spectrometry; MALDI-TOF/MS, matrix-assisted laser desorption ionization-time of flight mass spectrometry; MRT, mean residence time; NEP-24.11, neutral endopeptidese 24.11; PBS, phosphate buffered saline; PCR, polymerization chain reaction; PEG, polyethylene glycol; PK, pharmacokinetic; SD, Sprague-Dawley; $T_{1/2}$, elimination half-life; TFA, trifluoroacetic acid; TLC, size-exclusion thin layer gel-chromatography; T_{max}, time to reach C_{max}; V_{dss}, volume of distribution at steady state.

Keywords: Glucagon-like peptide-1 analog, Type 2 diabetes, Aggregation, Bacterial streptococcal G strain 148, Long half-life

1. Introduction

Glucagon-like peptide-1 (GLP-1) is a member of the incretins family of gastrointestinal peptide hormones [1]. The main physiological action of GLP-1 is to potentiate insulin secretion. This action is highly glucose-dependent, and is mediated via its receptor in pancreatic β-cells. In other organs, GLP-1 shows pharmaceutically important actions including gastric emptying and appetite regulation. Therefore, GLP-1 is an attractive drug target for the treatment of type 2 diabetes and obesity, and intense studies have been conducted. GLP-1 is produced by proglucagon processing, and is stored in secretory granules [2,3]. It is subsequently released through exocytosis in response to increased intracellular calcium level. GLP-1 itself has a very short half-life (less than 2 minutes) as it rapidly undergoes enzymatic degradation and renal clearance in the circulation. Like other peptide drugs, the design of injectable GLP-1 analogs has therefore been centered on achieving a long-lasting action [4-6].

A number of approaches have been adopted to overcome the intrinsically short half-life of GLP-1 [7]. Among them, macromolecularization is considered to be one of the promising strategies [8-10]. Previous efforts have focused on conjugation of peptides to polyethylene glycol (PEG) or to natural proteins, such as Fc and albumin, or on modification of the parent peptide with protractors that can reversibly bind to serum albumin (half-life of 19 days in human). Indeed, GLP-1-based drugs, including albiglutide and liraglutide have exemplified recent success in this field [11]. These conjugated peptides have long in vivo half-lives of several ten hours to several weeks, allowing once daily to once monthly dosing. Nevertheless, there still exists a need for new macromolecularization technologies that would allow wider applicability to various peptide drug candidates, as will be later discussed in this manuscript.

In the course of our program towards new GLP-1 analogs, we conducted screening of [Ser^{8}]-GLP-1 analogs using the C-terminal helix 3 of the albumin binding domain 3 of protein G from bacterial Streptococcal G strain 148 (G148-ABD3), and have found **6** as a long-acting GLP-1 analog with enhanced aggregate formation by self-association [12-14]. Herein, we present the pharmacological profiles of **6** and show experimental data for oligomeric forms of **6**, which may account for its extended in vivo half-life.

2. Materials and methods

2.1 Materials

Native GLP-1 (7-36) was purchased from Peptide Institute, Inc. (Osaka, Japan). Radioactive [^{125}I]-GLP-1 (7-36), [Ser^{8}]-GLP-1 (7-36) and Liraglutide were purchased from Bachem Peninsula (CA, USA). Exenatide was purchased from Sigma-aldrich (MO, USA). Tritium-labeled **6** was synthesized by Sekisui Medical Co., Ltd (Tokyo, Japan) using tritium tyrosine as described below.

2.2. Peptide synthesis

The synthesis of peptides **1-10** was carried out in a solid phase using Fmoc chemistry and Wang PEG resin with HBTU/DIEA as coupling reagents. Deprotection of Fmoc groups was achieved by treatment with 20% piperidine in dimethyl formamide (DMF) for 5 min. This treatment was repeated three times to ensure complete deprotection. Coupling was carried out under shaking at room temperature for 30 min. The resin was washed with DMF after each deprotection or coupling (three times in total) and used for the next reaction. This cycle was repeated to synthesize the appropriate peptide building blocks and subsequently the target peptides. The target peptides were cleaved from the resin and deprotected in a mixture of meta-cresol, thioanisole, triisopropylsilane, and trifluoroacetic acid (TFA) (1.8/0.5/0.3/13 v/v/v/v) at room temperature for 1.5 h. The resin was filtered off, and the filtrate was evaporated under reduced pressure. The crude target peptides were precipitated with diethyl ether, collected, and suspended in 50% aqueous acetonitrile containing 0.1% TFA. They were then freeze-dried and purified by reverse-phase high performance liquid chromatography (HPLC) on a C18 column in a gradient mode in aqueous acetonitrile containing 0.1% TFA, and their integrity was confirmed by MALDI-TOF/MS. Analytical HPLC and LTQ-Orbitrap were performed on an LC10A System (Shimadzu) and an Acquity UPLC (Waters), respectively. HPLC profiles were obtained using a C18 column (4.6 × 250 mm, pore size 100Å, particle size 0.5 μm) at a constant flow rate of 1.0 mL/min, in a gradient mode with eluent A, 0.1% aqueous TFA and eluent B, 0.1% TFA in acetonitrile (ACN), or eluent A, 0.05% aqueous TFA and eluent B, 0.05% TFA in acetonitrile. Monitoring at a wavelength of 220 nm indicated that the purified peptides were ≥95% pure. The analytical results of purity and LTQ-Orbitrap are given in Table 1.

2.3. Cell lines

Mouse insulinoma MIN6 cell line was donated by Professor Jun-ichi Miyazaki (Osaka

University, Osaka, Japan). The MIN6 cells were maintained in Dulbecco's modified Eagle's medium containing 25 mM glucose supplemented with 15% heat-inactivated fetal bovine serum (FBS), 50 units/mL penicillin, 50 μg/mL streptomycin, 4 mM L-glutamine, and 5 μL β-mercaptoethanol at 37 °C (5% CO_2 and 95% air).
Chinese hamster ovary (CHO-K1) cells over-expressing hGLP-1 receptors (GLP-1R) were constructed in-house. The pIRES vector (Clonetech Inc., CA, USA) harboring a cDNA of hGLP-1 receptor (hGLP-1R; NM 002062) was transfected into CHO-K1 cells by lipofection. The hGLP-1R-expressing clone cells were then selected using 400 μg/mL geneticin containing 10% FBS-Ham's F-12 medium. Geneticin-resistant clones were next isolated and amplified. mRNA levels of hGLP-1R in these clones were measured by real time polymerization chain reaction (PCR), and the clone that retained the highest expression level of hGLP-1R mRNA was used for cyclic adenosine monophosphate (cAMP) production assays.

2.4. Animals

Diabetic db/db mice, ICR mouse, and Sprague-Dawley (SD) rats were purchased from Charles River Laboratories Japan, Inc. (Kanagawa, Japan), and housed under standard conditions with a 12-h light/dark cycle and free access to water and a commercial diet (CRF-1, Oriental Yeast, Japan) for at least 5 days. All animal procedures were approved by the Sanwa Kagaku Kenkyusho Institutional Animal Care and Use Committee, and conducted in accordance with institutional guidelines for the Conduct of Animal Experiments in Research Institutions under the Jurisdiction of the Ministry of Health, Labor, and Welfare" (2006).

2.5. Plasma stability

Peptides plasma stability was assessed in SD rat or human plasma. Rat blood was collected via the abdominal aorta of 8-week old SD rats. The fresh rat plasma was mixed with a solution of a peptide analog (100 μM) to a final concentration of 0.5 μM, and the mixture was incubated at 37 °C. Samples were taken at 8 and 48 h, quenched in ice-cold ethanol and centrifuged (12,000 rpm, 4 °C, 10 min), and the supernatants were analyzed by LC/MS (LTQ-Orbitrap, Thermo-Fischer). The remaining percentages of each peptide for the two time-points (8 and 48 h) were calculated from their peak areas relative to zero-time point sample, taken as 100% and used to determine peptide plasma stability. Human blood samples were ethically sourced, and their use was in accord with

the terms of the informed consents. Experiments using human samples were conducted as described above, and the results are given in Table 4.

2.6. Insulin secretion in MIN6 cell line

MIN6 cells were seeded in 96 well plates and cultured for 48 h at 80 % confluence on the experimental day. The seeded cells were incubated in Hepes-Krebs ringer (KRH) buffer containing 2 mM glucose for 1 h and again incubated in KRH buffer with 10, 30, 100, 300 and 1,000 pM of each analog and glucose (15 mM) for 1 h. The concentrations of insulin in cell culture supernatants were measured by enzyme-linked immunosorbent assay (ELISA) (AKRIN-011T, Shibayagi Co., Ltd., Gunma, Japan). EC_{50} values were calculated by GraphPAD Prism.

2.7. Glucose lowering effects in diabetic db/db mice

Peptide **6**, **8**, **10**, [Ser^8]-GLP-1 (7-36) or vehicle (saline) was subcutaneously administered to 9-week old male diabetic db/db mice at a dose of 12.5 nmol/kg or 50 nmol/kg. Blood samples were collected from the tail vein at 0, 1, 2, 4, and 6 h after administration, and centrifuged. Plasma glucose concentrations were measured using Glucose-test Wako (Wako Pure Chemical Industries, Ltd., Osaka, Japan).

2.8. GLP-1 receptor agonistic activity

Cellular cAMP production of **6** and liraglutide in mouse insulinoma βTC6 cells was assayed by CEREP (France). Human GLP-1 receptors expressing CHO-K1 cells were seeded in 96 well plates at a density of 8.0 × 103 cells per well. After 48-h culture, the cells were washed two times with hanks-balanced salt solution (HBSS). Assay buffer (0.5% BSA, 1mM IBMX, 20 μM Ro201724 in HBSS was then added to each well, and the plates were incubated for 15 min at 37 °C. Peptide **6** or liraglutide (final concentration; 1 pM to 3 nM) in assay buffer was loaded onto each well, and the plates were incubated for another 30 min at 37 °C. The cells were lysed using assay/lysis buffer, and cAMP production was measured by ELISA Kit (cAMP-Screen System, Applied Biosystems, CA, USA). EC_{50} values for both analogs were calculated using GraphPAD Prism(GraphPad softwear, Inc.).

2.9. GLP-1 receptor ligand binding assay

Human GLP-1 receptor membrane preparation (hGLP-1R, ChemiSCREEN® Membrane Preparation Recombinant Human GLP-1, Millipore, MA, USA) was purchased and used for the receptor binding assay. For the saturation binding experiment, hGLP1-R was incubated for 90 min at room temperature with increasing amounts of [^{125}I]-GLP-1 (7-36) and final concentrations ranging from 0 to 1 nM (assay buffer; 50 mM HEPES, pH 7.4, 5 mM $MgCl_2$ 1 mM $CaCl_2$, 0.2% BSA). To determine non-specific binding, a similar experiment was conducted using 1 μM GLP-1 (7-36) to block hGLP1-R. For the competitive binding experiment, hGLP1-R was incubated for 90 min at 25 °C with various concentrations of **6** or liraglutide (final concentration; 1 pM to 10 μM) in the presence of 0.25 nM of [^{125}I]-GLP-1 (7-36) in assay buffer (50 mM HEPES, pH 7.4, 5 mM $MgCl_2$, 1 mM $CaCl_2$) containing 0.1% BSA or 4% BSA. The mixture was then filtered through a GF/B glass fiber filter (Whatman) pre-soaked with 0.33% polyethyleneimine (PEI) using a vacuum filter holder (Millipore), and the filters were washed with 3 mL of buffer (50 mM HEPES, 500 mM NaCl, 0.1% BSA). The washing was repeated three times, and the filters were dried, and their radioactivity was measured using Cobra Gamma Counter 5010 (Perkin-Elmer). Data were analyzed using GraphPad Prism (GraphPad softwear, Inc.), and inhibition curves were fitted to a four-parameter logistic equation to determine IC_{50} values.

2.10. Pharmacokinetic (PK)

Peptide **6** was suspended in saline and administered intravenously or subcutaneously to male SD rats (n = 4) at the dose of 0.01 mg/kg. Blood samples were collected via the jugular vein using a heparinised syringe at 0.083, 0.25, 0.5, 1, 2, 4, 6, 8, 10, 12 and 24 h postdose. The plasma was obtained by centrifugation (1,500 × g, 4 °C, 10 min) of the samples at 4 °C and stored at −70 °C until analysis. Plasma concentrations of **6** were determined using LC/MS, and its pharmacokinetic parameters were calculated using non-compartmental analysis (WinNonlin Professional, Version 5.2.1; Pharsight Corporation). Bioavailability was calculated by dividing $AUC_{0-\infty}$ after subcutaneous administration by $AUC_{0-\infty}$ after intravenous administration.

2.11. Serum protein binding

Blood was collected via the abdominal aortas of 6-week old ICR mice and 7-week old SD rat using syringes containing EDTA-2K. Blood samples were left to stand for 30 min at

room temperature, and the sera were isolated by centrifugation (1,800 × g, 4 °C, 15 min). Human serum albumin (HAS) was purchased from Sigma-aldrich (MO, USA) and diluted with phosphate buffered saline (PBS) to prepare assay solutions. Tritium-labeled **6** (414 MBq/mg) was diluted in ethanol-water (6:4) with various concentrations of each biologic (final concentrations of 10, 100, 1000 nM) and incubated at 37 °C for 1 h. Control incubations of [^{3}H]-**6** in PBS without any biologic were also performed. Aliquots of the mouse serum, rat serum, human serum, HSA and PBS samples were placed in polycarbonate ultracentrifuge tubes (200 μL, duplicate), and centrifuged (200,000 × g, 4 °C, 6 h). The supernatants were then collected (50 μL × 2 tubes) in scintillation vials. Each serum or HSA sample was mixed with 10 mL of the scintillator Hionic-Fluor (Perkin Elimer) to measure the radioactivity using a liquid scintillation counter (3100TR, Perkin Elmer). Protein binding was determined from the observed counts and calculated using the equation below.

Protein binding (%) = (1 – S/P) × 100

P: Radioactivity concentration in supernatant collected from centrifuged PBS solution (dpm/mL)

S: Radioactivity concentration in supernatant collected from centrifuged serum solution (dpm/mL)

2.12. Neutral endopeptidese 24.11 (NEP-24.11) stability assay

Human recombinant NEP-24.11 was purchased from R&D systems, Inc. (MN, USA). NEP-24.11 (0.04 μg/mL) in reaction buffer (50 mM HEPES, 50 mM NaCl, pH 7.4) was pre-incubated for 5 min at 37 °C. GLP-1 (7-36) or **6** (final concentration; 2.5 μM) was then added, and the samples were collected at 4 and 8 h after the addition. Enzyme reactions of the collected samples were terminated by addition of a mixture of ice-cold ethanol and 1.6% formic acid, and these samples were stored at −20 °C until LC/MS analysis. The remaining percentage of each analog was calculated from the peak area relative to zero-time point sample taken as 100%.

2.13. Sedimentation velocity analytical ultracentrifugation

This experiment was conducted by Katakura industries Co., Ltd. (Tokyo, Japan). Peptide **6** was dissolved in 10 mM PBS at a final concentration of 100 μM. The sample (400 μL) was loaded into an analytical ultracentrifugation cell, and sedimentation velocity was measured out at 20 °C and 50,000 rpm using an XL-A Ultracentrifuge

systems (Beckman). Absorbance and interference data were collected simultaneously. Sedimentation coefficient and molar mass were analyzed by SEDFIT software.

2.14. Size-exclusion thin layer gel-chromatography (TLC)

Radioactive [^{125}I]-**6** was administered subcutaneously at a dose of 4 nmol/kg to a male SD rat (n = 1). Blood samples were collected 4 h postdose. Plasma was obtained by centrifugation of the samples at 4 °C and immediately loaded onto the gel layer. Separately, [^{125}I]-**6** (350 dpm/5 μL) was mixed with SD rat blank plasma and incubated for 4 h at 37 °C, after which it was immediately used as a control lane in the chromatography.

Sephadex G-100 (GE healthcare) gel suspensions were prepared in 0.01% HBSS. Glass plates (30 × 30 cm) were coated with a 0.9 mm thick layer of sephadex by means of thin-layer spreader. Pre-equilibration of gels was conducted in solvent moisture vessels over 8 h, then thin-layer gel plates were laid down at a slight tilt between a buffer tank (upper side) and a filter paper pad (lower side). Each sample was applied to upper edge of the gel plate. The solvent was supplied from the buffer tank through a Whatman filter paper. Development was monitored by bromophenol blue spot, and protein staining performed with colloidal gold. Radioactivity of the plasma sample was detected using Bioimaging analyzer BAS2000 (Fujifilm).

2.15. Statistical analysis

Significant difference and confidence interval were calculated by EXSAS software (CAC Croit Corporation).

3. Results

3.1. Rat plasma stability and insulinotropic activity

Preliminary screening was carried out using two 10- and 12-residues C-terminal albumin-binding domain 3 (ABD3) (**2** and **1**) and GLP-1 (Table 2). Both peptides **1** and **2** had insulinotropic activity comparable to that of GLP-1 and greatly improved plasma stability with half-lives of more than 48 h, while the stability of GLP-1 was below the lower limit of detection, i.e. within 8 h.

As to dipeptidyl peptidase-IV (DPP-IV) resistant [Ser^{8}]-GLP-1 (7-35) analog peptides, a

series of truncated ABD3 were prepared, and each fragment was connected to [Ser^{8}]-GLP-1 (7-35). Except for **7**, all [Ser^{8}]-GLP-1 analog peptides remained unchanged in rat plasma for 48 h and had good to excellent insulinotropic activity in MIN6 cells.

3.2. Glucose-lowering effects in db/db mice

Taking the number of residues into account, smaller peptides **6**, **8**, and **10** were evaluated for their glucose-lowering effect in db/db mice. The three peptides were given subcutaneously at a dose of 12.5 nmol/kg, and blood glucose levels were monitored for 6 h after administration (Table 3). Only **6** showed a significant glucose-lowering effect throughout the study, while **8** produced a significant difference in total blood glucose AUC compared to the vehicle control. Compared to [Ser^{8}]-GLP-1, the sustained glucose-lowering effect of **6** was observed when given at 50 nmol/kg (Fig. 1).

3.3. Functional and binding assays for GLP-1 receptor

To confirm that **6** is a potent GLP-1 analog with long in vivo half-life based on albumin binding, additional experiments to determine in vitro properties and PK parameters of **6** were conducted. Peptide **6** had mouse GLP-1R agonistic activity in a cAMP functional assay with an EC_{50} value of 1.2 nM, which is consistent with the data obtained in MIN6 cells assay. Peptide **6** also showed hGLP-1R agonistic activity with an EC_{50} value of 0.13 nM and had a binding affinity for hGLP-1R with an IC_{50} values of approximately 12 nM in a competitive binding assay using [^{125}I]-GLP-1. Moreover, peptide **6** showed greatly enhanced stability in human plasma, compared to native GLP-1 (Table 4). Unlike **6**, liraglutide was influenced by BSA concentration in binding assay (Table 5).

3.4. PK parameters

In rats, intravenous administration of **6** resulted in an extended half-life of 5.4 h, relative to the reported half-life of [Ser^{8}]-GLP-1 (7-36) (several minutes in pigs) [15], with small distribution volume (Vdss) (Table 6). Peptide **6**, given subcutaneously given, reached half C_{max} within 1 h, and its concentration-time profile indicated a further extended half-life of 5.8 h with good bioavailability (64%). However, albumin binding study using [^{3}H]-**6** revealed thatonly 70-80% of **6** bound to human plasma protein at concentrations ranging from 10 to 1000 nM. Likewise, the binding of **6** to HSA was as low as 55-62% (Table 7). In the NEP-24.11 stability study using human recombinant

NEP-24.11, a relatively slow degradation of GLP-1 (7-36) was observed, while **6** was found to be a poorer substrate for NEP-24.11 than GLP-1 (7-36) (Table 8).

3.5. Sedimentation velocity analytical ultracentrifugation and TLC

Sedimentation velocity analytical ultracentrifugation using XL-A was performed to determine whether the stock solution of **6** contained oligomeric species (Fig. 2). Three peaks of 1.34, 2.46, and 3.34 S were present in the stock solution, corresponding to a trimer, hexamer and decamer, respectively. While the hexamer and decamer were found to be main oligomeric forms, no monomer was detected. This led us to investigate the presence of oligomers in vivo. Radioactive [^{125}I]-**6** was administered to an SD rat at a dose of 4 nmol/kg, and the plasma sample collected 4 h postdose was directly applied to TLC on Sephadex G-100 with 0.01% tween/HBSS as eluent. Peptide **6** and its radioactive analog yielded a single band at molecular weight of approximately 44 KDa and a large band at more than 75 KDa along with faint bands (lanes 1 and 2), respectively. This indicated that both peptides **6** and [^{125}I]-**6** formed oligomeric spcies. In the in vivo sample lane 3, a band consistent with [^{125}I]-**6** was observed along with plasma protein bands, which is virtually identical to the reference lane 6 of a mixture of rat plasma and [^{125}I]-**6** (Fig. 3).

4. Discussion

Our initial strategy for macromolecularization was based on modification using albumin binding protractors. Albumin contains multiple binding sites and can transport a variety of endogenous and exogenous substances including fatty acids, ions such as calcium and magnesium, hormones, amino acids, toxins, and drugs. Moreover, albumin has recently been shown to be more permeable to glomerular filtration barriers than was once thought, indicating that albumin reabsorption in the proximal tubules is very important for its homeostasis [16-19]. In this reabsorption process, albumin is considered to bind to membrane proteins, such as the megalin/cubilin receptor complex and the neonatal Fc receptor (FcRn) [19]. Collectively, ideal albumin binding protractors can enhance the therapeutic potential of parent drugs without having any effects of their bound albumin on the transport properties and physiological regulation. G148-ABD can bind to albumin without interfering with its binding to FcRn [20]. In addition, G148-ABD shows excellent albumin binding affinity across species and contains three homologous albumin binding domains (G148-ABD 1-3). Of these domains,

G148-ABD3 is the most extensively studied [20]. For example, Jonsson et al. have identified a femtomolar affinity variant, ABD035, by constructing a library of the C-terminal helix 3 (15 residues) using phage-display technologies in combinatorial fashion [22]. Furthermore, Ghosh et al. used ABD035 as protractor to generate a potent analog of exenatide, a GLP-1 mimetic, with high metabolic stability [23].

As a logical extension, we initially surveyed the shortest peptide fragment (helix 3) of G148-ABD3. Enhancement of glucose-stimulated insulin secretion from pancreatic β-cells is the fundamental role of GLP-1-based drugs. To sieve test peptides **1**-**10**, we used this convenient screening system with MIN6 cells, which endogenously express GLP-1R, in combination with rat plasma stability assay. DPP-IV-resistant analog [Ser^{8}]-GLP-1 (7-35) [24] was used as backbone peptide for the second round screening, considering that the DPP-IV cleaves peptide bonds after the Pro or Ala residues penultimate to the N-terminal 3-6 and is mainly responsible for the short half-life of GLP-1 in circulation [25]. As consistent with the preliminary screening based on rat plasma and MIN6 cells assays, **6** had potent mouse and human GLP-1R agonistic activity, with excellent binding affinity for human GLP-1R. Peptide **6** also showed enhanced stability in human plasma and an extended half-life of 5.4 h with good bioavailability in rats, resulting in prolonged therapeutic effects in diabetic mice. However, the low level of plasma protein binding of **6** came as a surprise. Thus, the data obtained from the albumin binding study using [^{3}H]-**6** are consistent and explain the phenomenon observed in the comparative GLP-1R binding assay. That is, unbound **6**, which is responsible for binding to GLP-1R, was present in the assay medium at concentrations more than 100-fold higher than those of unbound liraglutide, based on liraglutide binding to human plasma protein (>99%). Nevertheless, analog **6** showed greatly enhanced stability in human plasma (100 % after 48 h) [26]. Overall, unlike liraglutide, the enhanced stability of **6** is not attributed to its protein binding ability. One may speculate that this enhanced stability is attributed to resistance to NEP-24.11, another enzyme responsible for proteolysis of endogenous GLP-1 [27]. Proteolysis occurred at the six sites of GLP-1 between 27–28 (-E-F-) and 31–32 (-W-L-), followed by 15–16 (-D-V-), 18–19 (-S-Y-), 19–20 (-Y-L-), and 28–29 (-F-I-). Indeed, **6** possesses all cleavage sites, and its appendage is at the C-terminal close to the favored sites. Therefore, steric hindrance of the appendage and/or increased size of **6** itself may have played a role in NEP-24.11 resistance. In fact, **6** showed excellent NEP-24.11 resistance in our experiment. Notwithstanding, we felt that this hypothesis was unlikely due to the following two aspects. First, although [Ser^{8}]-GLP-1 is known to be DPP-IV resistant, its in vivo half-life is only several minutes [15], indicating that the enhanced stability

may be largely attributed to DPP-IV resistance. In addition, it is reported that in vivo inhibition of NEP-24.11 alone does not improve the insulinotropic effect of infused GLP-1 [15]. Second, judging from the reported structure-activity relationships of NEP-24.11-resistant C-type natriuretic peptides, the small difference in size between the three peptides **6**, **8**, and **10** is unlikely to be a decisive factor for NEP-24.11 resistance [28].

As mentioned above, GLP-1 is stored in secretory granules. Interestingly, it has been suggested that GLP-1 in the granules is in an amyloid-like aggregation state that serves as a very stable depot for extended preservation [2]. This has experimentally been recognized by the fact that chemically synthesized GLP-1 has aggregation propensity to form oligomeric species. This aggregation was initially considered to be heparin-mediated [29], and later suggested to be pH-dependent [30], although the precise mechanism remains to be investigated. Zapadka et al. have shown that the population of oligomeric species decreases under slightly basic conditions (pH 7.5 to 8.5), leaving unassociated proteins as the main species [30]. Since the likelihood of **6** being aggregated cannot be ruled out, we examined whether **6** formed aggregates by self-association. In fact, it is well known that a charged amino acids residue in a peptide can drive aggregation, and **6** has three charged residues, i.e. K (Lys), D (Asp), and E (Glu), in the appendage moiety. Expectedly, the results obtained from the analytical ultracentrifugation and TLC indicate that **6** formed large oligomers in solution and suggest that **6** remains oligomeric even in the circulation, which accounts for its extended in vivo half-life.

Therapeutic peptides (up to 50 amino acids) show high efficacy in the treatment of various disorders of globally prevalent diseases, and are now recognized as an important class of therapeutics. More than 60 peptides have so far been approved in the US with the global sales of 25 of them reaching US$14.7 billion in 2011 [31]. Currently, approximately 140 and more than 500 peptides are being developed in clinical and preclinical stages, respectively [32]. These numbers are expected to grow owing to emerging technologies such as multi-functionalization and cell-penetration [33-35]. As peptide drugs are widely used, their need for repeated administration, i.e. injection, has become a critical issue in the treatment of chronic diseases, thereby limiting the utility of peptide drugs. Conjugation of peptides to PEG as well as the albumin binding are the most promising technologies for extending peptide drugs half-lives. Very recently, PEGylated proteins have been reported to induce unwanted anti-PEG antibodies and complement activation [36]. The presence of anti-PEG antibodies leads to rapid clearance of the PEGylated protein, and PEG-induced complement activation is

believed to cause severe anaphylaxis, from which approximately 0.02% of patients died in the EMERALD trials, resulting in withdrawal of peginesatide from the market in 2013 [37]. At present, the EMA recommends that additional > 4-week pre-clinical toxicity studies are conducted on PEGylated drug candidates before clinical studies. In addition, it is a major concern that attachment of molecular protractors frequently results in a decrease in potency of the parent peptide [38]. Even in case of small molecule protractors, such as fatty acid side chains, the length, position, and composition of the fatty acid affect both the potency and protraction. Moreover, the choice of the spacer between the backbone peptide and the fatty acid is also detrimental [4,5].

The present work shows the possible enhancement of medium-sized oligopeptides aggregation propensity and highlights the potential advantages of peptide aggregates for long-acting peptide drugs. Peptides aggregation may be associated with amyloid-β fibrils, which are the main cause of neurodegenerative disorders, including Alzheimer's disease [2]. In addition, peptides propensity to aggregation is likely to be a considerable drawback in the development, manufacturing, and commercialization of peptide drugs [39,40]. Notwithstanding the drawbacks of peptide aggregation, further toxicity and PK-PD studies of **6** across various species would be very informative and their results will be reported elsewhere.

Disclosures

The authors declare no financial or otherwise conflicts of interest.

Acknowlegements

We thank Tomohiro Shigemori, Katsura Tsukamoto, Miyuki Tamura, Takayo Murase, Shinji Furuta, and Yoshiyuki Furuta for their comments and data production. We also thank Chika Otani and Asako Ohara for their experimental support.

References

[1] C. de Graaf, D. Donnelly, D. Wootten, J. Lau, P.M. Sexton, J.L. Miller, J.-M. Ahn, J.

Liao, M.M. Fletcher, D. Yang, A.J.H. Brown, C. Zhou, J. Deng, M.-W. Wang, Glucagon-like peptide-1 and its class B G protein–coupled receptors: A long march to therapeutic successes, Pharmacol. Rev. 68 (2016) 954–1013.

[2] S.K. Maji, M.H. Perrin, M.R. Sawaya, S. Jessberger, K. Vadodaria, R.A. Rissman, P. S. Singru, KP.R. Nilsson, R. Simon, D. Schubert, D. Eisenberg, J. Rivier, P. Sawchenko, W. Vale, R. Riek, Functional amyloids as natural storage of peptide hormones in pituitary secretory granules, Science 325 (2009) 328–332.

[3] S. Poon, N.R. Birkett, S.B. Fowler, B.F. Luisi, C.M. Dobson, J. Zurdo, Amyloidogenicity and aggregate cytotoxicity of human glucagon-like peptide-1 (hGLP-1), Protein Pept. Lett. 16 (2009) 1548–1556.

[4] K. Madsen, L.B. Knudsen, H. Agersoe, P.F. Nielsen, H. Thøgersen, M. Wilken, N.L. Johansen, Structure-activity and protraction relationship of long-acting glucagon-like peptide-1 derivatives: Importance of fatty acid length, polarity, and bulkiness, J. Med. Chem. 50 (2007) 6126-6132.

[5] J. Lau, P. Bloch, L. Schäffer, I. Pettersson, J. Spetzler, J. Kofoed, K. Madsen, L.B. Knudsen, J. McGuire, D.B. Steensgaard, H.M. Strauss, D.X. Gram, S.M. Knudsen, F.S. Nielsen, P. Thygesen, S. Reedtz-Runge, T. Kruse, Discovery of the once-weekly glucagon-like peptide-1 (GLP-1) analogue semaglutide, J. Med. Chem. 58 (2015) 7370−7380.

[6] M. Lorenz, A. Evers, M. Wagner, Recent progress and future options in the development of GLP-1 receptor agonists for the treatment of diabesity, Bioorg. Med. Chem. Lett. 23 (2013) 4011–4018.

[7] L. Di, Strategic approaches to optimizing peptide ADME properties, AAPS J. 17 (2015) 134–43.

[8] T. Arvedson, J. O'Kelly, B.-B. Yang, Design rationale and development approach for pegfilgrastim as a long-acting granulocyte colony-stimulating factor, BioDrugs 29 (2015) 185–198.

[9] D. Cuevas-Ramos, M. Fleseriu, Pasireotide: A novel treatment for patients with acromegaly, Drug Design Develop. Ther. 10 (2016) 227–239.

[10] A. Brønden, F.K. Knop, M.B. Christensen, Clinical pharmacokinetics and pharmacodynamics of albiglutide, Clin Pharmacokinet. 56 (2017) 719–731.

[11] H. Courtney, R. Nayar, C. Rajeswaran, R. Jandhyala, Long-term management of type 2 diabetes with glucagon-like peptide-1 receptor agonists, Diabetes. Metab. Syndr. Obes. 10 (2017) 79–87.

[12] E. van der Linden, P. Venema, Self-assembly and aggregation of proteins, Curr. Opin. Coll. Interface Sci. 12 (2007) 158–165.

[13] N. Stephanopoulos, J.H. Ortony, S.I. Stupp, Self-assembly for the synthesis of functional biomaterials, Acta Materialia 61 (2013) 912–930.

[14] H. Acar, S. Srivastava, E.J. Chung, M.R. Schnorenberg, J.C. Barrett, J.L. LaBelle, M. Tirrell, Self-assembling peptide-based building blocks in medical applications, Adv. Drug Deliv. Rev. 110–111 (2017) 65–79.

[15] A. Plamboeck, J.J. Holst, R.D. Carr, C.F. Deacon, Neutral endopeptidase 24.11 and dipeptidyl peptidase IV are both mediators of the degradation of glucagon-like peptide 1 in the anaesthetised pig, Diabetologia 48 (2005) 1882–1890.

[16] A. Tojo, S. Kinugasa, Mechanisms of glomerular albumin filtration and tubular reabsorption, Int. J. Nephrol. (2012) ID 481520.

[17] M.J. Moeller, V. Tenten, Renal albumin filtration: Alternative models to the standard physical barriers, Nat. Rev. Nephrol. 9 (2013) 266–277.

[18] L.E. Dickson, M.C. Wagner, R.M. Sandoval, B.A. Molitoris, The proximal tubule and albuminuria: Really!, J. Am. Soc. Nephrol. 25 (2014) 443–453.

[19] K.M.K. Sand, M. Bern, J. Nilsen, H.T. Noordzij, I. Sandlie, J.T. Anderse, Unraveling the interaction between FcRn and albumin: Opportunities for design of albumin-based therapeutics, Front. Immunol. 5 (2015) article 682.

[20] J.T. Andersen, R. Pehrson, V. Tolmachev, M.B. Daba, L. Abrahmse´n, C. Ekblad, Extending half-life by indirect targeting of the neonatal Fc receptor (FcRn) using a minimal albumin binding domain, J. Biol. Chem. 286 (2011) 5234–5241.

[21] J. Nilvebrant, S. Hober, The albumin-binding domain as a scaffold for protein engineering, Comput. Struct. Biotechnol. J. 6 (2013) e201303009.

[22] A. Jonsson, J. Dogan, N. Herne, L. Abrahmse´n, P. Nygren, Engineering of a femtomolar affinity binding protein to human serum albumin, Protein Eng. Des. Sel. 21 (2008) 515–27.

[23] O.E. Levy, C.M. Jodka, S.S. Ren, L. Mamedova, A. Sharma, M. Samant, L.J. D'Souza, C.J. Soares, D.R. Yuskin, L. J. Jin, D.G. Parkes, K. Tatarkiewicz, S.S. Ghosh, Novel exenatide analogs with peptidic albumin binding domains: potent anti-diabetic agents with extended duration of action, PLoS One. 9 (2014) e87704.

[24] C.F. Deacon, L.B. Knudsen, K. Madsen, F.C. Wiberg, O. Jacobsen, J.J. Holst, Dipeptidyl peptidase IV resistant analogues of glucagon-like peptide-1 which have extended metabolic stability and improved biological activity, Diabetologia 41 (1998) 271–278.

[25] R. Mentlein, B. Gallwitz, W.E. Schmidt, Dipeptidyl-peptidase IV hydrolyses gastric inhibitory polypeptide, glucagon-like peptide-l (7-36) amide, peptide histidine methionine and is responsible for their degradation in human serum, Eur. J.

Biochem. 214 (1993) 829-835.

[26] A. Plum, L.B. Jensen, J.B. Kristensen, In vitro protein binding of liraglutide in human plasma determined by reiterated stepwise equilibrium dialysis, J. Pharm. Sci. 102 (2013) 2882–2888.

[27] K. Hupe-Sodmann, G.P. McGregor, R. Bridenbaugh, R. GöSke, B. GöSke, H. Thole, B. Zimmermann, K. Voigt, Characterisation of the processing by human neutral endopeptidase 24.11 of GLP-1 (7-36) amide and comparison of the substrate specificity of the enzyme for other glucagon-like peptides, Regul Pept. 58 (1995)149–156.

[28] D.J. Wendt, M. Dvorak-Ewell, S. Bullens, F. Lorget, S.M. Bell, J. Peng, S. Castillo, M. Aoyagi-Scharber, C.A. O'Neill, P. Krejci, W.R. Wilcox, D.L. Rimoin, S. Bunting, Neutral endopeptidase-resistant C-type natriuretic peptide variant represents a new therapeutic approach for treatment of fibroblast growth factor receptor 3–related dwarfism, J. Pharmacol. Exp. Ther. 353 (2015) 132–149.

[29] N.N. Jha, A. Anoop, S. Ranganathan, G.M. Mohite, R. Padinhateeri, S.K. Maji, Characterization of amyloid formation by glucagon-like peptides: role of basic residues in heparin-mediated aggregation, Biochemistry 52 (2013) 8800–8810.

[30] K.L. Zapadka, F.J. Becher, S. Uddin, P.G. Varley, S. Bishop, A.L.G. dos Santos S.E. Jackson, A pH-induced switch in human glucagon-like peptide‐1 aggregation kinetics, J. Am. Chem. Soc. 138 (2016) 16259−16265.

[31] A.A. Kaspar, J.M. Reichert, Future directions for peptide therapeutics development, Drug Disc. Today 18 (2013) 807-817.

[32] K. Fosgerau, T. Hoffmann, Peptide therapeutics: current status and future directions, Drug Disc. Today 20 (2015) 122-128.

[33] T.A.S. Aguirre, D. Teijeiro-Osorio, M. Rosa, I.S. Coulter, M.J. Alonso, D.J. Brayden, Current status of selected oral peptide technologies in advanced preclinical development and in clinical trials, Adv. Drug Delivery Rev. 106 (2016) 223–241.

[34] A. Komin, L.M. Russell, K.A. Hristova, P.C. Searson, Peptide-based strategies for enhanced cell uptake, transcellular transport, and circulation: Mechanisms and challenges, Adv. Drug Delivery Rev. 110-111 (2017) 52–64.

[35] B. Finan, C. Clemmensen, T.D. Müller, Emerging opportunities for the treatment of metabolic diseases: Glucagon-like peptide-1 based multi-agonists, Mol. Cell. Endocrinol. 418 (2015) 42–54.

[36] J.J.F. Verhoef1, J.F. Carpenter, T.J. Anchordoquy, H. Schellekens, Potential induction of anti-PEG antibodies and complement activation toward PEGylated therapeutics, Drug Disc. Today 19 (2014) 1945–1952.

[37] T. Kaushik, M.M. Yaqoob, Lessons learned from peginesatide in the treatment of anemia associated with chronic kidney disease in patients on dialysis, Biologics 7 (2013) 243–246.

[38] S.C. Penchala, M.R. Miller, A. Pal, J. Dong, N.R. Madadi, J. Xie, H. Joo, J. Tsai, P. Batoon, V. Samoshin, A. Franz, T. Cox, J. Miles, W.K. Chan, M.SP. Park, M.M. Alhamadsheh, A biomimetic approach for enhancing the in vivo half-life of peptides, Nat Chem Biol. 11 (2015) 793–798.

[39] C.J. Roberts, Therapeutic protein aggregation: mechanisms, design, and control, Trends Biotechnol. 32 (2014) 372−380.

[40] C.J. Roberts, Protein aggregation and its impact on product quality, Curr. Opin. Biotechnol. 30 (2014) 211–217.

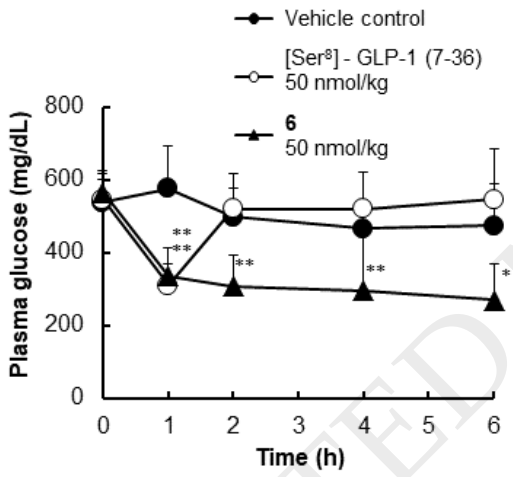

Fig. 1. Glucose-lowering effects of **6** and [Ser^8]-GLP-1 (7-36) in diabetic db/db mice. Data are expressed as the mean + SD of seven animals. *$p < 0.05$, **$p < 0.01$, ***$p < 0.001$ vs. vehicle control.

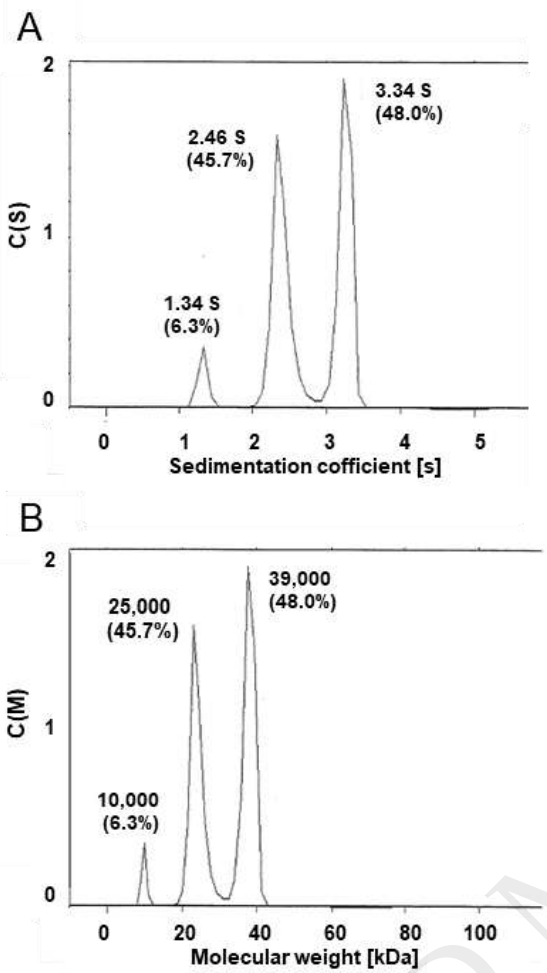

Fig. 2. Sedimentation velocity analytical ultracentrifugation of the stock solution of **6**. Analytical ultracentrifugation was performed using Beckman Optima XL-A. Sedimentation coefficient (A) and molecular weight (B) for the stock solution of **6** were determined by SEDFIT software.

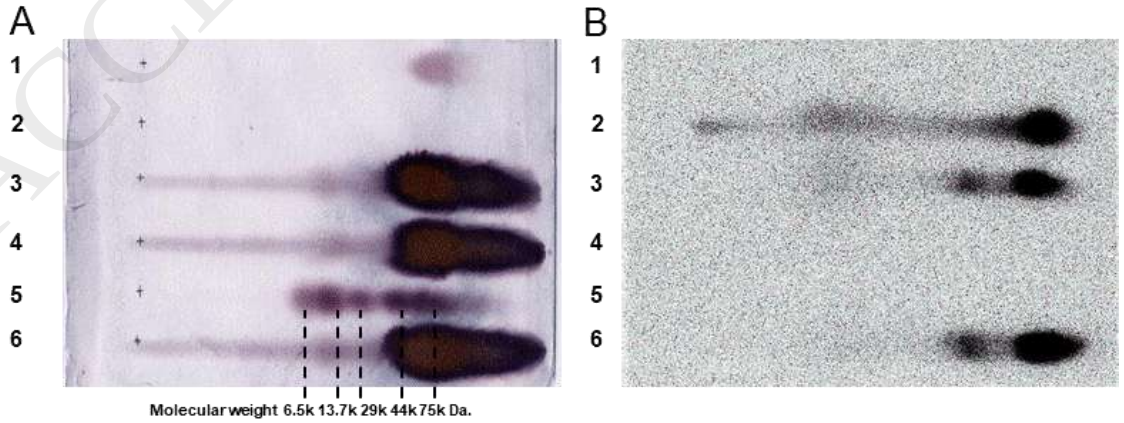

Fig. 3. Size-exclusion thin layer gel chromatography of the plasma sample obtained from [^{125}I]-**6**-treated rat. The plate was developed with 0.01% HBSS. The spots were detected by staining with colloidal gold (A), followed by Bioimage Analyzer for 120 h (radioactivity) (B). Lane 1, **6**; lane 2, [^{125}I]-**6**; lane 3, rat plasma (4 h after subcutaneous administration of [^{125}I]-**6** at the dose of 4 nmol/kg); lane 4, rat blank plasma; lane 5, molecular marker proteins (Aprotinin, Ribonucleaase A, Carbonic anhydrase, Ovalbumin, Conalbumin); lane 6, rat blank plasma plus [^{125}I]-**6**.

Table 1

Chemical purity and identity of the peptides **1** – **10**.

Peptide	Sequence	Purity %	Calculated mass (monoisotopic)	Observed mass (deconvoluted)
1	HAEGTFTSDVSSYLEGQAAKEFIAWLVKG-GVKALIDEILAA-NH_2	100[a]	4333.263	4333.264
2	HAEGTFTSDVSSYLEGQAAKEFIAWLVKG-KALIDEILAA-NH_2	100[a]	4177.173	4177.171
3	HSEGTFTSDVSSYLEGQAAKEFIAWLVKG-AKTVEGVKALIDEILAA-NH_2	96.4[b]	4877.549	4877.551
4	HSEGTFTSDVSSYLEGQAAKEFIAWLVKG-VEGVKALIDEILAA-NH_2	95.4[b]	4577.369	4577.358
5	HSEGTFTSDVSSYLEGQAAKEFIAWLVKG-EGVKALIDEILAA-NH_2	97.2[b]	4478.301	4478.294
6	HSEGTFTSDVSSYLEGQAAKEFIAWLVKG-GVKALIDEILAA-NH_2	96.1[b]	4349.258	4349.264
7	HSEGTFTSDVSSYLEGQAAKEFIAWLVKG-VKALIDEILAA-NH_2	95.2[b]	4292.237	4292.250
8	HSEGTFTSDVSSYLEGQAAKEFIAWLVKG-KALIDEILAA-NH_2	95.0[b]	4193.168	4193.176
9	HSEGTFTSDVSSYLEGQAAKEFIAWLVKG-LIDEILAA-NH_2	95.1[b]	3994.036	3994.061
10	HSEGTFTSDVSSYLEGQAAKEFIAWLVKG-IDEILAA-NH_2	96.4[b]	3880.952	3880.979

[a] HPLC condition, detection UV 220 nm, eluent A-0.1% TFA/H_2O, B-0.1% TFA/ACN, gradient 30% to 90% solvent B in 30 minutes, flow rate 1.0 mL/min.

[b] HPLC condition, detection UV 220 nm, eluent A-0.05% TFA/H_2O, B-0.05% TFA/ACN, gradient 20% to 90% solvent B in 34 minutes, flow rate 1.0 mL/min.

Table 2

Stability and insulinotropic potency of peptides **1**-**10**.

Peptide	Sequence	Stability in rat plasma (%)		Insulinotropic action	
		8 h	48 h	% of maximum	EC_{50} (nM)
GLP-1 (7-36)-NH_2	HAEGTFTSDVSSYLEGQAAKEFIAWLVKGR-NH_2	0	-	100	0.12
1	GLP-1 (7-35)-GVKALIDEILAA-NH_2	102	76	99	0.55
2	GLP-1 (7-35)-KALIDEILAA-NH_2	97	75	106	0.09
[Ser ^{8}]-GLP-1 (7-36)-NH_2	HSEGTFTSDVSSYLEGQAAKEFIAWLVKGR-NH_2	17	0	83	0.18
3	[Ser ^{8}]- GLP-1 (7-35)- AKTVEGVKALIDEILAA-NH_2	107	116	105	0.21
4	[Ser ^{8}]- GLP-1 (7-35)- VEGVKALIDEILAA-NH_2	99	92	83	-
5	[Ser ^{8}]- GLP-1 (7-35)- EGVKALIDEILAA-NH_2	96	68	109	-
6	[Ser ^{8}]- GLP-1 (7-35)- GVKALIDEILAA-NH_2	104	93	118	1.7
7	[Ser ^{8}]- GLP-1 (7-35)- VKALIDEILAA-NH_2	115	113	44	-
8	[Ser ^{8}]- GLP-1 (7-35)- KALIDEILAA-NH_2	77	117	115	-
9	[Ser ^{8}]- GLP-1 (7-35)- LIDEILAA-NH_2	113	95	82	-
10	[Ser ^{8}]- GLP-1 (7-35)- IDEILAA-NH_2	97	95	120	0.27

Data are expressed as the mean value (n=3). -, Not measured.

Table 3

Comparison of plasma glucose-lowering effects of **6**, **8** and **10** in diabetic db/db mice.

Peptide	% of Vehicle control Glucose AUC 0-t (mg·h/dL)	
	1 h	6 h
6	86.9 ± 8.5*	83.0 ± 9.3**
8	94.6 ± 6.6	93.3 ± 7.3*
10	98.6 ± 5.9	101 ± 10.9

Data are expressed as the mean ± standard deviation (SD) of seven animals. *$p < 0.05$, **$p < 0.01$ vs. vehicle control.

Table 4

Stability of GLP-1, [Ser ^{8}]-GLP-1 and **6** in human plasma.

Peptide	**S**tability in human plasma (%)	
	8 h	48 h
GLP-1（7-36）-NH_2	0	0
[Ser^8] - GLP-1（7-36）-NH_2	37.6	0
6	99.2	100

Data are expressed as the mean value (n = 3).

Table 5

Functional and binding abilities of **6** and liraglutide.

Peptide	cAMP production EC_{50} (nM)		[^{125}I]-GLP-1 (7-36) binding IC_{50} (nM)		IC_{50} ratio (0.1% BSA / 2% BSA)
	Mouse	Human	0.1% BSA	2% BSA	
6	1.2	0.131	12.71	11.68	1.09
Liraglutide	0.74	0.109	1.25	7.12	0.18

Data are expressed as the mean value in duplicate or triplicate.

Table 6

PK parameters of **6** in SD rats.

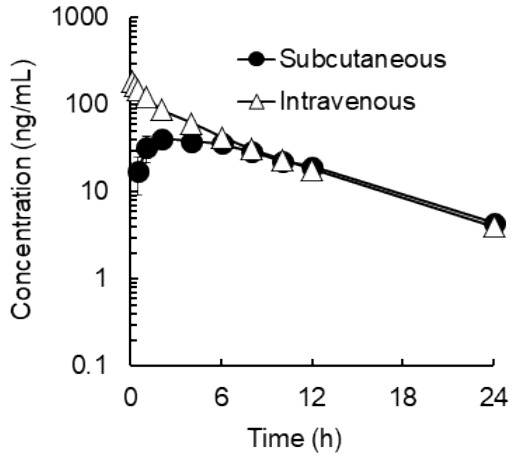

Parameters	Subcutaneous	Intravenous
*C*max (ng/mL)	43.0 ± 5.4	n.d.
*T*max (h)	4.0 ± 2.0	n.d.
$AUC_{0\text{-}t}$ (ng · h/mL)	510 ± 58	820 ± 19
$AUC_{0\text{-}C}$ (ng · h/mL)	548 ± 66	851 ± 23
*CL*p (mL/h/kg)	n.d.	11.8 ± 0.3
*V*dss (mL/kg)	n.d.	75.6 ± 1.7
$T_{1/2}$ (h)	5.8 ± 0.4	5.4 ± 0.3
MRT (h)	9.7 ± 0.7	6.4 ± 0.2
BA (%)	64.3 ± 7.7	n.d.

Data were obtained after subcutaneous or intravenous administration at a dose of 0.01 mg/kg, and are expressed as the mean ± standard deviation (SD) of five animals. n.d., not determined.

Table 7

Serum protein binding of ^{3}H-**6**.

Species	Concentration of ^{3}H-**6** (ng/mL)		
	10	100	1000
Mouse	82.0 ± 3.4	82.9 ± 1.6	81.8 ± 1.4
Rat	73.8 ± 6.0	81.9 ± 0.4	82.2 ± 0.5
Human	69.7 ± 13.0	75.4 ± 5.0	80.4 ± 1.6
HSA	55.3 ± 4.1	62.4 ± 4.2	57.6 ± 5.5

Data are expressed as the mean ±standard deviation (SD) in triplicate.

Table 8

Stability of GLP-1 and **6** for NEP-24.11.

Peptide	**S**tability in human

	plasma (%)	
	4 h	8 h
GLP-1 （7-36）-NH_2	59.4	29.4
6	90.5	84.4

Data are expressed as the mean value (n = 3).